Lattice approach to diquark condensation in dense matter

Simon Hands and Susan E. Morrison

(UKQCD Collaboration)

Department of Physics, University of Wales Swansea, Singleton Park, Swansea SA2 8PP, United Kingdom
(Received 27 July 1998; published 14 April 1999)

We present results of a Monte Carlo simulation of a three dimensional Gross-Neveu model with SU(2) $\otimes$ SU(2) chiral symmetry at a nonzero baryon chemical potential μ, corresponding to a nonzero baryon density. For μ sufficiently large there is a sharp transition between a phase where the chiral symmetry is broken by a condensate $\langle \bar{q}q \rangle$ and one where a scalar diquark condensate $|\langle qq \rangle| \neq 0$. Global U(1) baryon number symmetry may remain unbroken, however, due to the absence of long range order in the phase of $\langle qq \rangle$. There is also tentative evidence for the formation of a weaker pseudoscalar diquark condensate in the high density phase, which violates parity. [S0556-2821(99)01611-2]

PACS number(s): 11.30.Fs, 11.10.Kk, 11.15.Ha, 21.65.+f

I. INTRODUCTION

The properties and behavior of baryonic matter at high density have recently enjoyed renewed interest with the observation that the ground state even at densities sufficiently high for chiral symmetry to be restored may be far from trivial [1–3]. In brief, it is speculated that there is a regime of temperature and density for which the quarks have a large Fermi surface; kinetic considerations then suggest that if there is any attraction at all between quarks, then the free-particle vacuum is unstable with respect to condensation of diquark pairs from antipodal points on the surface, creating a gap between the Fermi energy and that of the lowest excited states. This is precisely a relativistic incarnation of the BCS instability in superconductors, with the diquarks playing the role of Cooper pairs.

The condensation phenomenon can be modelled by assuming the interaction between quarks is due to one-gluon exchange [1], or using effective four-fermion vertices resulting from the presence of instantons in the QCD vacuum [2,3]. A recent calculation using a phenomenologically inspired Nambu–Jona-Lasinio (NJL) model is given in [4]. Estimates of the gap energy are of order 100 MeV, comparable with the chiral condensate at zero density and temperature. It is intrinsically interesting in a field theoretic sense because the diquark condensate may not be invariant under global U(1) rotations associated with baryon number, and hence its formation be an example of spontaneous breaking of a vectorlike symmetry. The condensate is also a gauge nonsinglet, hence promoting a dynamical Higgs effect, and making some (or perhaps all [5]) of the gluons massive, leading to "color superconductivity." The pattern of symmetry breaking is predicted to be critically sensitive to the number of light quark flavors present [5]. Finally there may be interesting dynamical effects associated with the competition between chiral $\langle \bar{q}q \rangle$ and diquark $\langle qq \rangle$ condensates as the current quark mass m and baryon chemical potential μ are varied. Phenomenologically, diquark condensation and its generalizations could have implications for the distribution of strangeness observed in heavy ion collisions [6], and perhaps in the suppression of neutrino emission from neutron

star cores, resulting in slower cooling rates [2,6].

So far calculations have relied on model approximations to the QCD interaction, with *ad hoc* form factors introduced, for instance, to model the effect of asymptotic freedom, which should suppress the condensate at large Fermi momentum, and hence large μ. Many assumptions about the nature and origin of the qq interaction are necessary. This is a natural area, therefore, for numerical simulations of lattice QCD to make an impact. Recent simulations of QCD in a fixed gauge have found evidence for weak diquark binding at zero density [7]. Unfortunately, with $\mu \neq 0$, the Euclidean QCD path integral measure $\det M(\mu)$, where M is the fermion kinetic operator, is complex, making standard Monte Carlo simulation impossible. The most promising approach is to locate the zeros of the QCD grand canonical partition function in the complex fugacity plane avoiding the problem of the complex action by generating the statistical ensemble using $\det M(\mu=0)e^{-S_G}$ (where S_G is the gauge action) and reweighting with the factor $\det M(\mu \neq 0)/\det M(\mu=0)$ to achieve an overlap with the correct $\mu \neq 0$ ensemble. This method, though exact in principle, appears extremely slow to converge in practice, and the results, though promising, are far from definitive [8]. To date the lattice approach has only successfully been applied at nonzero density to toy field theories [9–11]. In this paper we present the first lattice study of diquark condensation in one such model, the Gross-Neveu (GN) model with SU(2) $\otimes$ SU(2) chiral symmetry formulated in $d = 2+1$ spacetime dimensions.

Which features of the GN model make it worth studying? In brief [12,13]; for sufficiently strong coupling the model exhibits dynamical chiral symmetry breaking at zero temperature and density, the spectrum of excitations contains both baryons (the elementary fermions), and mesons (composite fermion–antifermion states), which include a Goldstone mode, for $2 < d < 4$ the model has an interacting continuum limit, and when formulated on a lattice, the model has a real Euclidean action even for chemical potential $\mu \neq 0$, and hence can be simulated by standard Monte Carlo techniques.

Therefore the model displays much of the essential physics except for color confinement. Even such a simple theory

may be useful in addressing some of the issues raised above, including the behavior of competing condensates, and the full phase diagram in the (μ, T) plane once temperature $T > 0$. Simulations at $T = 0$ [10,11] have revealed a first order chiral symmetry restoring transition at $\mu_c \simeq m_f$, where m_f is the physical (i.e., constituent) fermion mass at $\mu = 0$; this is in marked contrast to the pathological behavior observed in approximations to QCD when the measure is held real, such as the quenched approximation, where $\mu_c \sim m_\pi/2$ [14].

In the next section we will describe the lattice model in detail, and identify which diquark operators we have studied using both lattice and continuum notation. Our simulations and results are described in Sec. III, and a short discussion given in Sec. IV.

II. THE LATTICE MODEL

A. Action and symmetries

The lattice model we have simulated has the following Euclidean path integral:

$$Z = \int D\sigma D\vec{\pi} \det(M^\dagger M[\sigma, \vec{\pi}]) \exp\left(-\frac{2}{g^2}(\sigma^2 + \vec{\pi} \cdot \vec{\pi})\right), \tag{1}$$

where σ and the triplet $\vec{\pi}$ are real auxiliary fields defined on the dual sites $\tilde{x}$ of a three dimensional Euclidean lattice. The determinant factor can be viewed as having been obtained by integrating over Grassmann variables $\chi, \bar{\chi}, \zeta, \bar{\zeta}$ with the following action:

$$S_{fer} = \bar{\chi} M[\sigma, \vec{\pi}] \chi + \bar{\zeta} M^*[\sigma, \vec{\pi}] \zeta \tag{2}$$

with

$$M_{xy}^{pq}[\sigma, \vec{\pi}] = \frac{1}{2} \delta^{pq} \left[(e^\mu \delta_{yx+\hat{0}} - e^{-\mu} \delta_{yx-\hat{0}}) \right.$$

$$+ \sum_{\nu=1,2} \eta_\nu(x)(\delta_{yx+\hat{\nu}} - \delta_{yx-\hat{\nu}}) + 2m\delta_{xy} \bigg]$$

$$+ \frac{1}{8} \delta_{xy} \sum_{\langle \tilde{x}, x \rangle} (\sigma(\tilde{x}) \delta^{pq} + i\varepsilon(x) \vec{\pi}(\tilde{x}) \cdot \vec{\tau}^{pq}). \tag{3}$$

The parameters are the bare fermion mass m, the chemical potential μ and the coupling g^2. The $\vec{\tau}$ are Pauli matrices with indices $p, q = 1, 2$. The symbols $\eta_\nu(x)$ denote the phases $(-1)^{x_0 + \cdots + x_{\nu-1}}$, $\varepsilon(x)$ the phase $(-1)^{x_0 + x_1 + x_2}$, and $\langle \tilde{x}, x \rangle$ the set of 8 dual lattice sites neighboring x. In this form we see that χ and ζ can be identified with isodoublet staggered lattice fermion fields defined on the sites x. The integration measure in Eq. (1) is manifestly real;[1] note that χ and ζ have opposite-signed couplings to the fields π_1 and π_3. It is

straightforward to integrate over the auxiliary fields σ and $\vec{\pi}$ to recover an action which contains fermions which self-interact via a four point interaction $\propto g^2$; more details are given for the corresponding four-dimensional model in [16].

In the limit $m \to 0$, the model is invariant under a global symmetry akin to the $SU(2)_L \otimes SU(2)_R$ of the continuum NJL model. Defining projection operators onto even and odd sublattices $\mathcal{P}_{e/o}$ by

$$\mathcal{P}_{e/o}(x) = \frac{1}{2}(1 \pm \varepsilon(x)), \tag{4}$$

we have

$$\chi \mapsto (\mathcal{P}_e U + \mathcal{P}_o V)\chi; \quad \bar{\chi} \mapsto \bar{\chi}(\mathcal{P}_e V^\dagger + \mathcal{P}_o U^\dagger)$$

$$\zeta \mapsto (\mathcal{P}_e V + \mathcal{P}_o U)\zeta; \quad \bar{\zeta} \mapsto \bar{\zeta}(\mathcal{P}_e U^\dagger + \mathcal{P}_o V^\dagger) \tag{5}$$

$$\Phi \equiv (\sigma \mathbb{1} + i\vec{\pi} \cdot \vec{\tau}) \mapsto V \Phi U^\dagger$$

with $U, V \in SU(2)$. Now for $T = \mu = 0$, a mean field treatment (which for a model with N flavors of χ and ζ is equivalent to the leading order of an expansion in $1/N$) shows that this $SU(2) \otimes SU(2)$ symmetry is spontaneously broken to $SU(2)_{isospin}$ by the generation of a condensate $\Sigma_0 = \langle \sigma \rangle = (2/g^2)\langle \bar{\chi}\chi \rangle$ and physical fermion mass $m_f = \Sigma_0$, the symmetry being broken for coupling $g^2 > g_c^2 \simeq 1.0$. Hence Σ_0 defines a physical scale in cutoff units: a continuum limit exists as $g^2 \to g_c^2$ from either phase. Quantum corrections to this picture can be calculated as higher order terms in the $1/N$ expansion, which is renormalizable about $g^2 = g_c^2$ [12,13]. The numerical results in this paper have been obtained for $N = 1$ and a value $g^2 = 2.0$, corresponding to a zero density theory deep in the broken phase, with $\Sigma_0 = 0.706(1)$ in units of inverse lattice spacing, i.e., rather far from the continuum limit.

We can also identify two other symmetries of Eqs. (1),(3), both of which hold even for $m \neq 0$. First, there is the global U(1) of baryon number:

$$\chi, \zeta \mapsto e^{i\alpha}\chi, \zeta; \quad \bar{\chi}, \bar{\zeta} \mapsto e^{-i\alpha}\bar{\chi}, \bar{\zeta}. \tag{6}$$

The chemical potential μ couples to the conserved charge associated with this symmetry. Next, there is a discrete parity symmetry appropriate to $2+1$ dimensions:

$$x = (x_0, x_1, x_2) \mapsto x' = (x_0, 1 - x_1, x_2)$$

$$\chi, \zeta(x) \mapsto (-1)^{x_1' + x_2'} \chi, \zeta(x');$$

$$\bar{\chi}, \bar{\zeta}(x) \mapsto (-1)^{x_1' + x_2'} \bar{\chi}, \bar{\zeta}(x') \tag{7}$$

$$\sigma(\tilde{x}) \mapsto \sigma(\tilde{x}'); \quad \vec{\pi}(\tilde{x}) \mapsto -\vec{\pi}(\tilde{x}'),$$

whence the identification of σ as scalar and π as pseudoscalar.

For $T, \mu \neq 0$ a mean field solution is also known [17,10], in which $\Sigma(\mu, T)$ is expressed in terms of Σ_0. At zero tem-

---

[1] Note also that $\det M = \det \tau_2 M^* \tau_2$ is real [15].

perature the basic feature is that Σ remains constant as μ is increased up to a critical value $\mu_c = \Sigma_0$, whereupon Σ falls sharply to zero (in the chiral limit), signalling a first order chiral symmetry restoring transition. Monte Carlo simulations [10] support this picture, even when massless Goldstone excitations (with the quantum numbers of the π field) are present, and N takes the minimal value $N = 1$ [11].

The reality of the measure in Eq. (1) is an artifact of our introducing conjugate flavors χ and ζ. It is worth discussing how the Monte Carlo simulation manages to reproduce the main features of the expected behavior of the model once $\mu \neq 0$, while similar simulations of QCD with quarks and conjugate quarks fail dramatically [14,18]. In brief, it is because interactions between χ and ζ are negligible so that a light bound $\chi\zeta$ state, which would carry baryon number, does not form. The strongest interactions are in the singlet channels $\chi\bar{\chi}$ and $\zeta\bar{\zeta}$, which are dominated by disconnected ''bubble'' diagrams in the $1/N$ expansion, and it is in these channels that Goldstone poles form [19]. Similarly, one might wonder how a diquark condensate, which is not invariant under the vectorlike U(1) global symmetry of baryon number, could ever form in a model with a real measure, since such a breaking is usually forbidden by the Vafa-Witten theorem [20]. The resolution is that the theorem does not hold for models with Yukawa couplings to scalar degrees of freedom, such as the coupling to σ in Eq. (3).

B. Constructing diquarks

Next we discuss the operators used to form diquark pairs. We begin by expressing the operators in terms of the lattice fields χ (we did not perform measurements in the ζ sector, but the results here are identical). In this study we have used four different local diquark operators:

$$NSS: \ \chi^p(x)\chi^p(x), \quad NSP: \ \varepsilon(x)\chi^p(x)\chi^p(x)$$

$$SS: \ \chi^p(x)\tau_2^{pq}\chi^q(x), \quad SP: \ \varepsilon(x)\chi^p(x)\tau_2^{pq}\chi^q(x).$$
$$(8)$$

Operators NSS and NSP are symmetric in both spatial and isospin indices, and so would only form a nonzero condensate if extra flavors are introduced, i.e., $N > 1$. In this case the operator could be written, with the indices i,j running from 1 to N, $\frac{1}{2}\chi_i\varepsilon_{ij}\chi_j$. For $N = 1$ this vanishes identically, but as described below, the diagram which would contribute for $N \geq 2$ can also be measured on an ensemble generated with $N = 1$ in a generalization of the quenched approximation; we will refer to such operators as *nonspectral diquarks*. Operators SS and SP, on the other hand, are symmetric in space but antisymmetric in isospin, and hence can form even for $N = 1$; we will refer to these as *spectral diquarks*. States NSS and SS are even under parity (7), and so will be called *scalar*, while NSP and SP are odd, and hence *pseudoscalar*. Note that NSS and NSP are not invariant under the chiral rotations (5), or indeed under the remnant isospin symmetry in the chirally broken phase, and all four diquark operators not invariant under the U(1) of baryon number (6).

To gain further insight it is useful to transform to a basis in which continuumlike spinor indices are shown. The recipe for staggered fermions in three dimensions is well known [21]. First we make a unitary transformation to fields u and d defined on a lattice of twice the spacing of the original, with site labels y:

$$u^{\alpha a}(y) = \frac{1}{4\sqrt{2}} \sum_A \Gamma_A^{\alpha a} \chi(A;y);$$

$$d^{\alpha a}(y) = \frac{1}{4\sqrt{2}} \sum_A B_A^{\alpha a} \chi(A;y). \tag{9}$$

The indices α, a each run from 1 to 2. Here A is a lattice vector with entries either 0 or 1, so that each site x on the original lattice corresponds to a unique combination of y and A. The 2×2 matrices Γ and B are defined by

$$\Gamma_A = \tau_1^{A_0}\tau_2^{A_1}\tau_3^{A_2}; \quad B_A = (-\tau_1)^{A_0}(-\tau_2)^{A_1}(-\tau_3)^{A_2}. \tag{10}$$

Now, with the definition

$$q^{\alpha a}(y) = \begin{pmatrix} u^\alpha(y) \\ d^\alpha(y) \end{pmatrix}^a, \tag{11}$$

we see that q may be interpreted as a four-component spinor operated on by Dirac matrices defined by

$$\gamma_i = \begin{pmatrix} & \tau_{i+1} \\ -\tau_{i+1} & \end{pmatrix} (i = 0,1,2); \quad \gamma_3 = \begin{pmatrix} & -i\mathbb{1} \\ i\mathbb{1} & \end{pmatrix};$$

$$\gamma_5 = \begin{pmatrix} & \mathbb{1} \\ \mathbb{1} & \end{pmatrix}, \tag{12}$$

with two flavors counted by the latin index a; this extra flavor degree of freedom is due to the species doubling inherent in the lattice approach. It is now possible to recast the fermion matrix (3) including the Yukawa interactions in continuumlike notation [21,13]. Here we will content ouselves with writing down expressions for the diquark operators (8) in the q basis:

$$NSS: \ -iq^T(\mathcal{C}\gamma_5 \otimes \tau_2 \otimes \mathbb{1})q, \quad NSP: \ -iq^T(\mathcal{C} \otimes \tau_2 \otimes \mathbb{1})q$$

$$SS: \ -iq^T(\mathcal{C}\gamma_5 \otimes \tau_2 \otimes \tau_2)q, \quad SP: \ -iq^T(\mathcal{C} \otimes \tau_2 \otimes \tau_2)q. \tag{13}$$

Here the first matrix in the direct product acts on the 4-spinor indices, the second on the implicit flavor space indexed by a, and the third on the explicit isospin degree of freedom indexed by p,q. The matrix $\mathcal{C}$ is the antiunitary charge conjugation matrix defined by $\mathcal{C}\gamma_\mu\mathcal{C}^{-1} = -\gamma_\mu^*$; in our explicit basis (12) $\mathcal{C} \equiv \gamma_0\gamma_2$. Denoting a symmetric state by s and an antisymmetric by a, we see operators NSS, NSP are $a \otimes a \otimes s = s$, and SS and SP $a \otimes a \otimes a = a$, corroborating our identification of spectral and nonspectral operators made earlier.

We can also rewrite the symmetries in the q basis. The $SU(2) \otimes SU(2)$ chiral symmetry (5) becomes

$$q_L \mapsto U q_L; \quad q_R \mapsto V q_R \quad \text{with} \quad q_{L/R} = \frac{1}{2}(1 \pm (\gamma_5 \otimes 1 \otimes 1))q,$$

$$(14)$$

the U(1) of baryon number (6)

$$q \mapsto \exp(i\alpha(1 \otimes 1 \otimes 1))q; \quad \bar{q} \mapsto \bar{q}\exp(-i\alpha(1 \otimes 1 \otimes 1)),$$

$$(15)$$

while the parity transformation (7) is now

$$q(x) \mapsto (\gamma_1 \gamma_5 \otimes 1 \otimes 1)q(x'); \quad \bar{q}(x) \mapsto \bar{q}(x')(\gamma_5 \gamma_1 \otimes 1 \otimes 1).$$

$$(16)$$

The parity assignments of the diquark operators (13) can be checked by observing that $\gamma_1 \gamma_5$ is a symmetric matrix.

III. SIMULATIONS

We have performed simulations of the model (1),(3) on $L_s^2 \times L_t$ lattices with bare mass $m = 0.01$ at a coupling $1/g^2 = 0.5$, with L_s varying between 8 and 24, and L_t between 24 and 40. The chemical potential μ was varied between 0 and 1.2, with a critical value for chiral symmetry restoration $\mu_c \simeq 0.65$. The simulation method is a standard hybrid Monte Carlo algorithm. The data presented here typically result from 100 measurements drawn from runs spanning $O(180)$ units of simulation time. We monitored the chiral condensate $\langle \bar{\chi} \chi \rangle$, and the baryon density n defined by

$$n = \frac{1}{2} \langle \bar{\chi}^p(x)e^\mu \chi^p(x+\hat{0}) + \bar{\chi}^p(x)e^{-\mu}\chi^p(x-\hat{0}) \rangle$$

$$\simeq \langle \bar{q}(\gamma_0 \otimes 1 \otimes 1)q \rangle \qquad (17)$$

using stochastic estimators.

To estimate diquark condensates we chose an indirect method: the two point function $\langle qq(0)\bar{q}\bar{q}(x) \rangle$ was measured as the expectation of the product of two fermion propagators as in QCD baryon spectroscopy, and the condensate extracted by assuming clustering at large spacetime separation, i.e.,

$$\langle qq(0)\bar{q}\bar{q}(x) \rangle = \langle qq(0)\bar{q}\bar{q}(x) \rangle_c + \langle qq \rangle \langle \bar{q}\bar{q} \rangle, \quad (18)$$

the latter term on the right being proportional to $|\langle qq \rangle|^2$. A nonzero condensate signal therefore shows up as a plateau in the timeslice correlator $G(t)$ at large time separation, and may be extracted by a fit of the form

$$G(t) = \sum_{x_1, x_2} \langle qq(0)\bar{q}\bar{q}(t,x_1,x_2) \rangle$$

$$= A \exp(-M_+ t) + B \exp(-M_-(L_t - t))$$

$$+ C^2(L_s)|\langle qq \rangle|^2, \qquad (19)$$

with $M_\pm$ the masses of forward and backward propagating diquark states, respectively. To perform the fit we used a least squares method taking account of correlations between different timeslices in the calculation of χ^2. The value of the
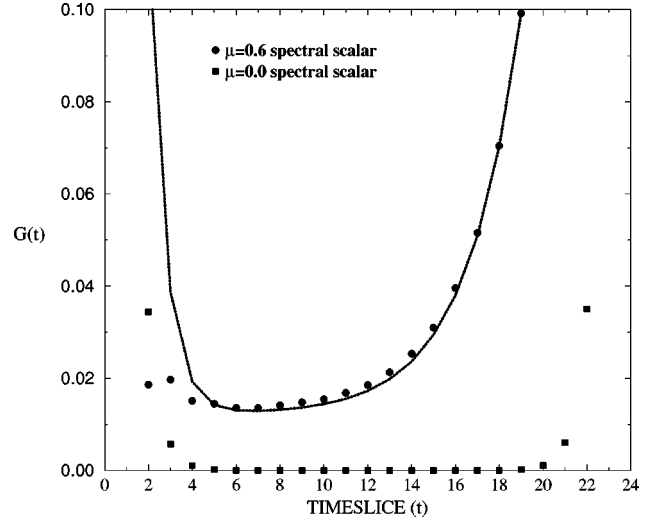

FIG. 1. Spectral scalar correlators for two values of μ in the broken phase on $16^2 \times 24$ lattices.

constant $C(L_s)$ is not determined *a priori*. Naively one expects $C = L_s$, and hence the plateau height to be an extensive quantity.

We found by measuring the chiral condensate that chiral symmetry is restored for chemical potential greater than $\mu_c \simeq 0.65$. The lattice virtually saturates with two χ quarks per site at $\mu = 1.5$ corresponding to a number density $n = 2$.

The spectral scalar propagators in the broken phase $\mu < \mu_c$ are shown in Fig. 1. For $\mu = 0.0$ the spectral scalar condensate signal is vanishing while for $\mu = 0.6$ it is very small but nonvanishing. We found no signal for the spectral pseudoscalar in the broken phase. The symmetric phase propagators and their fits are shown in Fig. 2. Noting the change in scale on the $G(t)$ axis and comparing with Fig. 1 we see that in the chirally symmetric phase a strong signal develops for the spectral scalar which increases with chemi-
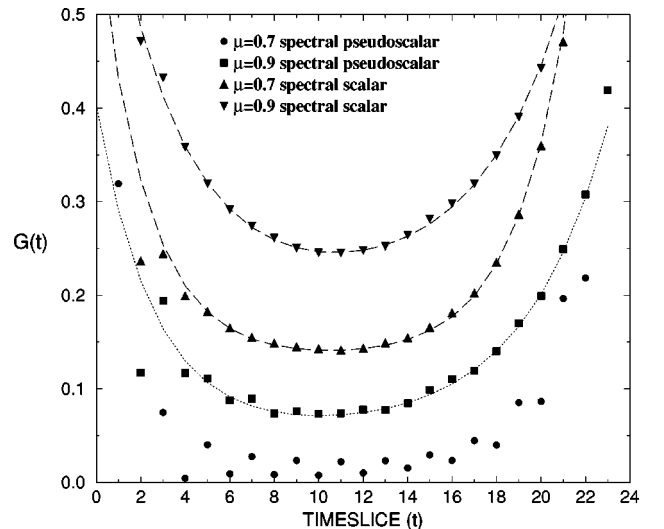

FIG. 2. Spectral scalar and pseudoscalar correlators and their fits for two μ values in the chirally symmetric phase on $16^2 \times 24$ lattices.
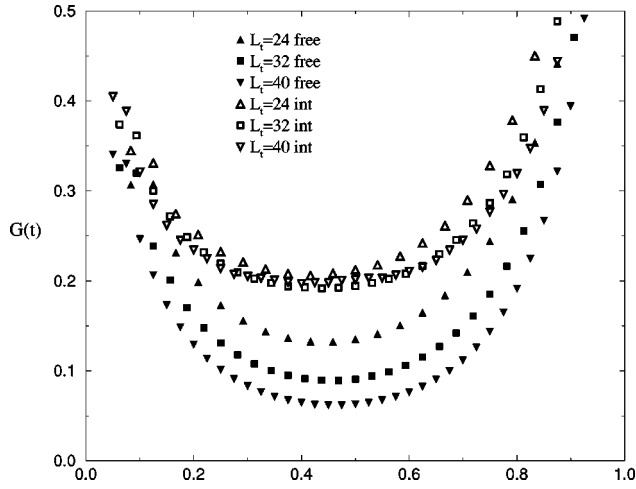
FIG. 3. Spectral scalar correlators measured on $16^2 \times L_t$ lattices at $\mu = 0.8$, together with the corresponding results for free fermions. Note that the t axis has been rescaled.
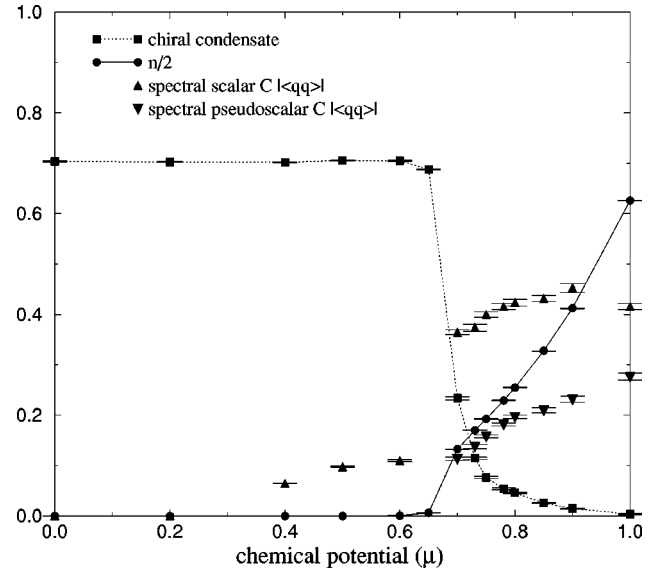

FIG. 4. Overview of the observables $\langle \bar{\chi}\chi \rangle$, n and SS and SP diquark condensate signals $C|\langle qq \rangle|$ as functions of μ, obtained on a $16^2 \times 24$ lattice, showing the onset of diquark condensation at $\mu_c \simeq 0.65$. As discussed in the text, the signal for the SS condensate for $\mu < \mu_c$, and the SP condensate at high density, are probably finite volume artifacts.

cal potential. The spectral pseudoscalar signal is weaker but distinctly nonzero and again increases with μ. The nonspectral propagators are not shown here although both the scalar and pseudoscalar closely follow the behavior of the spectral pseudoscalar.

The bulk of our results are from $16^2 \times 24$ lattices. However, to assess possible systematic effects arising from fitting the diquark propagators on lattices of finite temporal lattice extent L_t we repeated simulations at $\mu = 0.4$ on $16^2 \times 32$, and $\mu = 0.8$ on $16^2 \times 32$ and $16^2 \times 40$ lattices. The results at $\mu = 0.8$ are shown in Fig. 3, together with results obtained for diquark propagators constructed from free fermions (i.e., with $g^2 = 0$) on the same lattices with the same chemical potential (note that since the diquark is a boson, the oscillations normally expected of a free fermion propagator do not appear). The time axis has been normalized by L_t^{-1} to aid comparison. Note that the plateau height in the middle of the lattice is almost constant as L_t increases, consistent with $|\langle qq \rangle| \neq 0$, whereas in the free case the signal falls monotonically. We found that the fits to the spectral scalar correlator in the symmetric phase ($\mu = 0.8$) were very stable, yielding estimates for $C|\langle qq \rangle|$ of 0.425(1) for $L_t = 24$, 0.424(1) for $L_t = 32$, and 0.436(1) for $L_t = 40$. This is strong evidence for a nonvanishing condensate. The smaller parity violating signal, on the other hand, decreased by about 25% from 0.197(1) at $L_t = 24$, via 0.167(1) at $L_t = 32$, to 0.155(1) at $L_t = 40$. In the broken phase ($\mu = 0.4$) the spectral scalar $C|\langle qq \rangle|$ was 0.065(1) for $L_t = 24$ but consistent with zero on the $L_t = 32$ lattice suggesting that the $|\langle qq \rangle| \neq 0$ result in the broken phase is at least in part due to finite lattice size.

The trend in the diquark condensates as we pass from broken to symmetric phase is clear from Fig. 4. There is a critical value, $\mu_c \simeq 0.65$, at which the chiral $\langle \bar{q}q \rangle$ condensate falls sharply and the number density begins to rise from zero. The spectral scalar $C|\langle qq \rangle|$ condensate rises slowly from zero for $0.4 \lesssim \mu < \mu_c$, jumps upwards discontinuously close to μ_c, and continues to rise steadily. For $\mu > 1.0$ as the number density approached saturation the scalar qq propagators

became distorted and we were unable to achieve satisfactory fits.

The existence of a nonzero $\langle qq \rangle$ condensate in the broken phase could in principle convey physical information about the onset of a nucleon liquid type phase. A nonzero condensate implies that there is a Fermi surface and therefore nonzero number density. However, from the study with varying L_t discussed above, it is clear that further study is required to determine whether there is any nonzero signal associated with the onset of a nucleon liquid phase.

The spectral pseudoscalar $C|\langle qq \rangle|$ signal was consistent with zero for $\mu < \mu_c$ and no fits to the propagators were possible but for $\mu > \mu_c$ this condensate is non-zero and increases with μ. It is considerably smaller in magnitude than the spectral scalar. This pseudoscalar condensate is *parity violating*, and therefore it would be remarkable if the signal in the chirally symmetric phase were to remain nonzero in the large volume limit.

To determine the behavior with spatial volume we next performed a series of runs on $L_s^2 \times 24$ lattices at $\mu = 0.8$, with L_s varying from 8 to 24. To our surprise we found very little change as L_s increased, the fitted value of $C|\langle qq \rangle|$ more or less saturating for $L_s \geq 16$. Results for $L_s = 8, 16, 24$ are shown in Fig. 5, together with the fit for $L_s = 24$. For comparison we also plot the equivalent correlators for free fermions at $\mu = 0.8$; it is striking that for this case the trend as L_s increases is in the opposite direction. We conclude that the constant C is roughly independent of L_s; this puzzling behavior will be further discussed in the final section.

The diquark masses M_+ and M_- obtained from the fits to the spectral scalar qq propagator are plotted as a function of μ in Fig. 6. We found that the forward propagating M_+ states were more difficult to extract from the fits than the
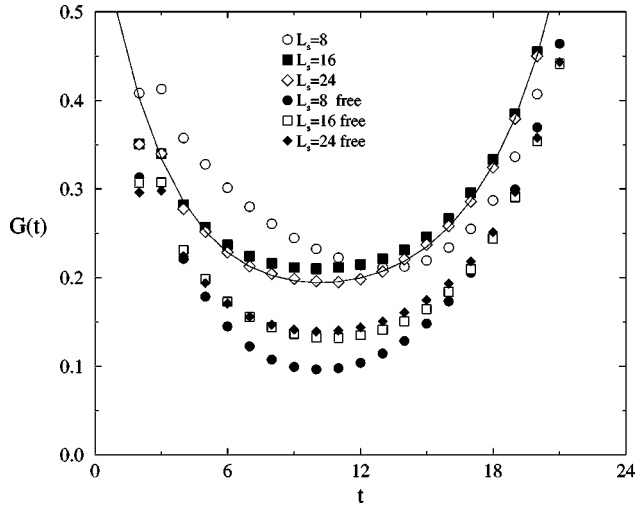
FIG. 5. Spectral scalar diquark correlator at $\mu = 0.8$ for both free and interacting quarks on $L_s^2 \times 24$ lattices.

FIG. 7. The three weaker diquark condensates $C|\langle qq \rangle|$ plotted in the high density phase as a function of μ.

backward propagating M_- states, as reflected in the size of the error bars. The trend in the data is clear with small masses in the symmetric phase and large masses in the broken phase. The approximate linear decrease of M_- with μ reflects a similar trend observed in the physical fermion mass m_f in previous simulations [11]. Notice that M_- is approximately constant for $\mu > \mu_c$. The observed qq states have masses around 0.3 which is light in comparison to the zero density fermion mass $m_f = \Sigma_0 \simeq 0.7$, which defines the ratio of physical to cutoff scales.

The spectral pseudoscalar and both nonspectral $C|\langle qq \rangle|$ condensates are plotted as a function of μ in Fig. 7. The signal for these three condensates is much weaker than the signal for the spectral scalar condensate. The parity-violating spectral pseudoscalar and the two nonspectral condensates are almost identical in magnitude and have remarkably similar behavior as a function of μ. We also remark that we have

observed no evidence for spontaneous violation of isospin on inspection of the fermion propagators.

To determine the effect of the bare quark mass on the $\langle qq \rangle$ condensates we performed simulations on $16^2 \times 24$ lattices for $m = 0.02, 0.05, 0.08, 0.1$ at $\mu = 0.8$. The values of the condensates were consistent within errors with the $m = 0.01$ result $C|\langle qq \rangle| = 0.424(7)$ for $m = 0.02, 0.05$ but the signal decreased by around 20% to 0.342(10) for $m = 0.08$ and by a further 20% to 0.272(6) for $m = 0.1$. In fact all of the diquark condensates decreased as we moved further from the chiral limit.

IV. SUMMARY AND OUTLOOK

We have simulated the 3D GN model with $SU(2) \otimes SU(2)$ chiral symmetry at nonzero chemical potential and found evidence suggestive of a diquark condensation, namely that the two-point correlation function exhibits clustering at large temporal separation. In order to quantify the measurement, however, it will be necessary to have a numerical estimate for the constant C in Eq. (19). We have up to now ignored the possible manifestations of fluctuations in the phase of the condensate. The spontaneous breaking of the $U(1)$ symmetry (6) usually implies the existence of a Goldstone mode associated with long wavelength fluctuations in the phase of the $\langle qq \rangle$ condensate; this is not accessible by the methods presented here, since $G(t)$ is real. However, in the absence of an explicit diquark source (analogous to a bare mass for the case of $\langle \bar{q}q \rangle$), one would expect large finite volume effects, generically proportional to $L^{-(d'-2)}$, where d' is the dimension of the effective field theory describing the fluctuations of the order parameter [22]. We therefore speculate that the effective field theory describing the spatial correlations of the diquark correlator has $d' = d - 1 = 2$, and that there is no long range order in the spatial directions [23]. A similar distinction between temporal and spatial correlations has been observed in instanton liquid models [3]. This would account for the volume independence
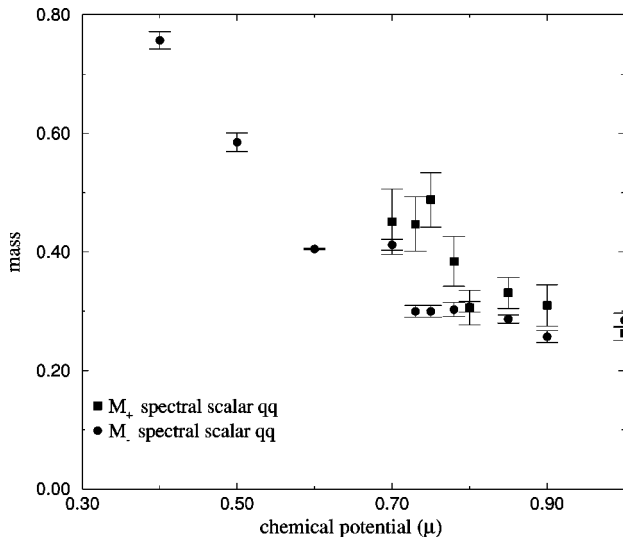

FIG. 6. Masses of forward and backward moving states M_+ and M_- obtained from fits to the spectral scalar propagators on a $16^2 \times 24$ lattice plotted as a function of μ.
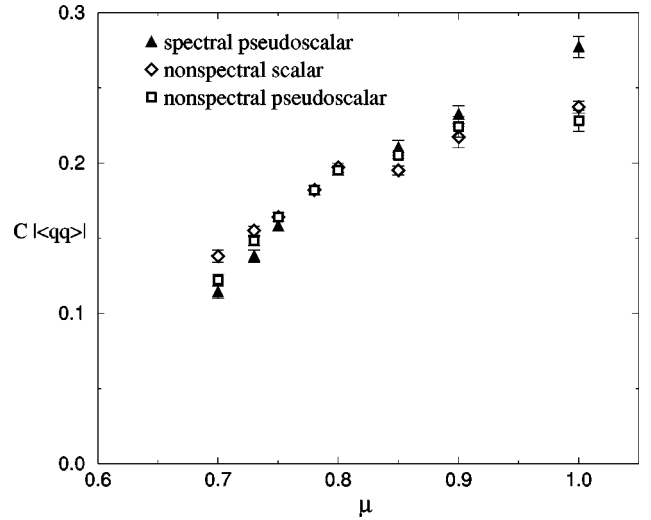
of C. Strictly speaking, therefore, we have not observed a true condensation. This interpretation of our results can be tested by simulations of the equivalent $3+1$ dimensional model [16], where we would expect long range order.

In a BCS condensation, only quark pairs with momenta $\pm p$ close to the Fermi surface contribute to the condensate. Therefore we expect that C^2, which must depend on the number of participating qq states, will be proportional to the area of the Fermi surface, i.e., $C^2 \propto \mu^{d-2}$. Note that the spectral scalar data in our work is well fitted by $C|\langle qq \rangle| \propto \sqrt{\mu}$ for $0.75 \lesssim \mu \lesssim 9$; fits over a wider range of μ, obtained from simulations closer to the continuum limit, would help to confirm this behavior. If we assume that $C \simeq O(\sqrt{\mu})$, we can claim to have detected a strong signal for a spectral scalar $|\langle qq \rangle|$ condensate in the chirally symmetric phase which is of the same order of magnitude as the chiral $\langle \bar{q}q \rangle$ condensate in the broken phase. This would imply that the energy gap associated with diquark condensation is $O(\Sigma_0)$ and hence support the predictions of [2–4].

We have observed a signal for $|\langle qq \rangle| \neq 0$ in the broken phase possibly associated with the onset of a nucleon liquid phase expected to occur for $\mu \lesssim \mu_c$, but further study of finite size effects is needed for confirmation. We have also detected a weak signal for a parity violating $|\langle qq \rangle|$ condensate in the chirally symmetric phase. This may be a three dimensional analogue of the axial diquark condensate reported in [2]. The remarks about finite size systematics apply here too; however this fascinating phenomenon could also be investigated by checking for the presence or absence of par-

ity doubling in the spectrum of spin-1 states. In a parity-symmetric vacuum we expect odd and even parity spin-1 states to be degenerate.[2] This can be observed in the spectroscopy of the 3D Thirring model [24].

The two-point method used here to measure the $\langle qq \rangle$ condensates requires the diquark operators (8) to be *local* in the χ fields; this excludes potentially interesting operators in this and related models. The introduction of an explicit diquark source to study the one-point function directly is thus desirable, both to calibrate our indirect two point function measurements, and to extend our study to other diquark operators and the $T \neq 0$ regime.

---

[2]This was pointed out to us by M. Teper.

[1] D. Bailin and A. Love, Phys. Rep. **107**, 325 (1984).

[2] M. Alford, K. Rajagopal, and F. Wilczek, Phys. Lett. B **422**, 247 (1998).

[3] R. Rapp, T. Schäfer, E. V. Shuryak, and M. Velkovsky, Phys. Rev. Lett. **81**, 53 (1998).

[4] J. Berges and K. Rajagopal, Nucl. Phys. **B538**, 215 (1999).

[5] M. Alford, K. Rajagopal, and F. Wilczek, Nucl. Phys. **B537**, 443 (1999).

[6] F. Wilczek, Nucl. Phys. **A642c**, 1c (1998).

[7] M. Hess, F. Karsch, E. Laermann, and I. Wetzorke, Phys. Rev. D **58**, 111502 (1998).

[8] I. M. Barbour, J. B. Kogut, and S. E. Morrison, Nucl. Phys. B (Proc. Suppl.) **53**, 456 (1997); I. M. Barbour, S. E. Morrison, E. G. Klepfish, J. B. Kogut, and M.-P. Lombardo, Phys. Rev. D **56**, 7063 (1997); Nucl. Phys. B (Proc. Suppl.) **60A**, 220 (1998).

[9] F. Karsch, J. B. Kogut, and H. W. Wyld, Nucl. Phys. B: Field Theory Stat. Syst. **B280**, 289 (1987).

[10] S. J. Hands, A. Kocić, and J. B. Kogut, Nucl. Phys. **B390**, 355 (1993).

[11] S. J. Hands, S. Kim, and J. B. Kogut, Nucl. Phys. **B442**, 364 (1995).

[12] B. Rosenstein, B. J. Warr, and S. H. Park, Phys. Rep. **205**, 59 (1991).

[13] S. J. Hands, A. Kocić, and J. B. Kogut, Ann. Phys. (N.Y.) **224**, 29 (1993).

[14] I. M. Barbour, N.-E. Behilil, E. Dagotto, F. Karsch, A. Moreo, M. Stone, and H. W. Wyld, Nucl. Phys. B: Field Theory Stat. Syst. **B275**, 296 (1986); C. T. H. Davies and E. G. Klepfish, Phys. Lett. B **256**, 68 (1991); M.-P. Lombardo, J. B. Kogut, and D. K. Sinclair, Phys. Rev. D **51**, 1282 (1995); **54**, 2303 (1996); R. Aloisio, V. Azcoiti, G. DiCarlo, A. Galante, and A. F. Grillo, Phys. Lett. B **435**, 175 (1998).

[15] M. A. Stephanov (private communication).

[16] S. J. Hands and J. B. Kogut, Nucl. Phys. **B520**, 382 (1998).

[17] B. Rosenstein, B. J. Warr, and S. H. Park, Phys. Rev. D **39**, 3088 (1989).

[18] A. Gocksch, Phys. Rev. D **37**, 1014 (1988); Phys. Rev. Lett. **61**, 2054 (1988); M. A. Stephanov, *ibid.* **76**, 4472 (1996).

[19] I. M. Barbour, S. J. Hands, J. B. Kogut, M.-P. Lombardo, and S. E. Morrison, hep-lat/9902033; S. E. Morrison, Nucl. Phys. **A642**, 269c (1998).

[20] C. Vafa and E. Witten, Nucl. Phys. **B234**, 173 (1984).

[21] C. J. Burden and A. N. Burkitt, Europhys. Lett. **3**, 545 (1987).

[22] P. Hasenfratz and H. Leutwyler, Nucl. Phys. **B343**, 241 (1990).

[23] N. D. Mermin and H. Wagner, Phys. Rev. Lett. **17**, 1133 (1966).

[24] L. Del Debbio, S. J. Hands, and J. C. Mehegan, Nucl. Phys. **B502**, 269 (1997).